Electrostatic and Hydrophobic Interactions Governing the Interaction and Binding of β-Lactoglobulin to Membranes†

Xiuqi Zhang, Ning Ge, and Timothy A. Keiderling*

Department of Chemistry, University of Illinois, 845 West Taylor Street (m/c 111), Chicago, Illinois 60607-7061

Received December 2, 2006; Revised Manuscript Received February 19, 2007

ABSTRACT: The role of electrostatic and hydrophobic interactions in the binding and penetration of β-lactoglobulin (βLG) to preformed lipid membranes was studied using various phospholipid micelles and vesicles. Zwitterionic lysophospholipid micelles are able to induce the β-sheet to α-helix transition, as judged by circular dichroism (CD), but the degree of transition is dramatically below and the amount of lipid required above that for anionic phospholipids with equivalent hydrocarbon chains. Anionic phospholipids with short hydrocarbon chains induce only low α-helical content in βLG as compared to phospholipids with the same head group but longer hydrocarbon chains. These results suggest that both electrostatic and hydrophobic interactions are indispensable in βLG−lipid interaction. Furthermore, air−water interface monolayer surface pressure and fluorescence anisotropy studies reveal that the membrane insertion of βLG strongly depends on the nature of phospholipids, given the identical headgroup, particularly lipid packing. These results are supported by urea denaturation and acrylamide fluorescence quenching tests and by the FTIR-ATR polarization results for βLG in multilayers on a surface. Under the same experimental conditions, the membrane binding and insertion of βLG as well as the stability of the βLG−lipid complexes can be enhanced by lowering the pH. Collectively, electrostatic interactions play a crucial role in all the processes involved in the βLG−lipid interaction, while the presence of hydrophobic interaction remains necessary. Finally, βLG biological function in the transport of fatty acids was tested by demonstrating the release of 2-AS from a 2-AS−βLG complex on binding to lipids.

Protein−membrane interaction has long been identified as a key element in understanding protein misfolding and consequent self-association- or aggregation-associated diseases, such as prion and amyloid diseases (*1*, *2*). The interaction between proteins and biological membranes as well as the kinetic mechanisms of any structural changes may vary from case to case. Generally, it has been thought that the insertion of a hydrophobic peptide or membrane protein segment into a lipid bilayer can be spontaneous, driven mainly by van der Waals attractions between the hydrophobic segments of the peptides and the hydrocarbon chains of the membranes. On the other hand, the interaction between water-soluble proteins and membranes mainly depends on the overall electrostatic interactions between the anionic lipid head groups and positively charged protein residues. Understanding the driving forces between proteins and lipids has been the focus of many studies (for reviews, see refs *3* and *4*). However, distinct roles of hydrophobic and electrostatic interactions in various peptide or protein−lipid binding processes remain elusive.

The lipocalin protein superfamily exhibits extraordinary diversity at the level of sequence and function. Generally, lipocalins are characterized by three molecular recognition properties: binding of small hydrophobic substances, binding to cell-surface receptors, and formation of complexes with other soluble macromolecules (*5*). Bovine β-lactoglobulin (βLG),[1] a lipocalin protein, is found in mammalian milk. It has been widely used in the food industry for its emulsifying and emulsion stabilizing properties, yet to date, its biological functions are still not clear (*6*). In the native state, βLG has a predominantly β-structure, consisting of one α-helix and nine antiparallel β-strands, forming a flattened β-barrel core which provides a binding site for fatty acids and other hydrophobic molecules (*7*). On the basis of the similarity of the structure and this substrate binding property to those of fatty acid-binding proteins, transportation of fatty acids has been assumed to be a reasonable biological function for βLG.

Secondary structure algorithms predict that βLG has a substantial propensity to form helix (*8*). Consistent with this, βLG exhibits a β-to-α transition in the presence of alcohols (*8*, *9*) and ionic surfactants (*10*, *11*). Some studies on the interaction of βLG with lipid membranes have reported that the interaction between βLG and anionic lipids depends on both the head group and the hydrophobic chain of the phospholipids (*12*−*14*). Our recent study (*14*) on the

† Supported in part by a grant for equipment purchases from the National Science Foundation (CHE00-0316014) and by a fellowship (to T.A.K.) from the John Simon Guggenheim Foundation.

* To whom correspondence should be addressed. E-mail: tak@uic.edu. Fax: (312) 996-0431. Phone: (312) 996-3156.

[1] Abbreviations: 2-AS, 2-(9-anthroyloxy)stearic acid; ATR, attenuated total reflectance; βLG, β-lactoglobulin; CD, circular dichroism; CMC, critical micelle concentration; DPG, dioctanoylphosphatidylglycerol; DMPG, dimyristoylphosphatidylglycerol; DMPC, dimyristoylphosphatidycholine; DSPG, distearoylphosphatidylglycerol; DOPG, dioleoylphosphatidylglycerol; FTIR, Fourier transform infrared; LPC, lysophosphatidylcholine; LPG, lysophosphatidylglycerol; DPH, 1,6-phenyl-1,3,5-hexatriene; TMA-DPH, 1-[4-(trimethylammonium)phenyl]-6-phenyl-1,3,5-hexatriene; SUVs, small unilamellar vesicles.

10.1021/bi602483p CCC: $37.00
Published on Web 04/04/2007

interaction of βLG with phospholipids (12-C hydrocarbon chains) revealed that anionic phospholipids induced non-native α-helix, the degree of which depended on the concentration and relative amount of anionic head groups in mixed lipid systems, since zwitterionic phospholipids alone did not induce helix, as supported by previous reports (*12*−*14*). Thus, electrostatic interaction appears to be a prerequisite for membrane binding of βLG, and factors associated with electrostatic interaction may have a strong effect on the βLG−lipid interaction. However, salt alone cannot induce any significant conformational transition in βLG, and the βLG−lipid interaction cannot be completely dissociated at high salt concentrations. Both suggest that the electrostatic interaction alone is not enough for membrane binding of βLG, implying that hydrophobic interactions must play some role in this process. The specific role of hydrophobic and electrostatic interactions for protein adsorption, binding, and insertion into lipid membranes as well as for the stability of the βLG−lipid complex is still not clear.

To address these questions, in this study, interactions of BLG with different phospholipid vesicles and micelles were studied with circular dichroism (CD), fluorescence, IR polarization, and monolayer insertion experiments in an effort to differentiate the roles of electrostatic and hydrophobic interactions in the stages of membrane binding of protein as well as in the stability of the protein−lipid complex. In addition, a possible biologic function of βLG in terms of fatty acid transport has been modeled with fluorescence quenching experiments.

EXPERIMENTAL PROCEDURES

Materials. Bovine βLG (catalog no. L 3908), crystallized three times and lyophilized, was purchased from Sigma (St. Louis, MO) and used without further purification. Dioctanoylphosphatidylglycerol (DPG), dimyristoylphosphatidylglycerol (DMPG), distearoylphosphatidylglycerol (DSPG), dioleoylphosphatidylglycerol (DOPG), dimyristoylphosphatidycholine (DMPC), lysophosphatidylcholine (LPC), and lysophosphatidylglycerol (LPG) were obtained from Avanti Polar Lipids, Inc. (Alabaster, AL). Fluorescent probes, 1,6-phenyl-1,3,5-hexatriene (DPH), 1-[4-(trimethylammonium)phenyl]-6-phenyl-1,3,5-hexatriene (TMA-DPH), and 2-(9-anthroyloxy)stearic acid (2-AS) were obtained from Molecular Probes (Eugene, OR). Other chemicals (phosphate salts and urea) were purchased from Sigma.

Lipid Micelles and Vesicles. Lysophospholipid micelles were prepared by directly dispersing the desired amount of lipid powder into 10 mM phosphate buffer (pH 4.6 and 6.8), followed by extensive vortexing and then sonication for ∼30 min in a water bath sonicator (Branson 2200, Branson Ultrasonics Corp., Danbury, CT). The critical micelle concentrations (CMCs) of lysophosphatidylcholine (LPC) and lysophosphatidylglycerol (LPG) in 10 mM phosphate buffer are ∼40 and ∼288 μM, respectively (*15*).

Small unilamellar vesicles (SUVs) were prepared by sonication as described previously (*14*). Briefly, the required amount of dried phospholipid powder was dispersed in 10 mM phosphate buffer (pH 4.6 and 6.8) and then was vortexed extensively. The resulting multilamellar liposome suspension was subjected to a freeze−thaw process and then sonicated in a bath until a clear suspension of small unilamellar vesicles was obtained. For the preparation of vesicles containing DPH and TMA-DPH with lipid:DPH (TMA-DPH) ratios of 250:1 (molar), lipids and DPH (TMA-DPH) were mixed in a $CHCl_3/CH_3OH$ (3:1, v/v) mixture and then dried and sonicated as described above. βLG was added to small unilamellar lipid vesicles or micelles in their liquid crystalline phases, and then the mixture was allowed to equilibrate for 1 h prior to the study of the resultant protein−lipid complexes. There were sample-to-sample variations in the spectral intensities, depending on preparation and lipid conditions; however, the CD spectra for samples prepared under strictly identical conditions effectively overlapped, and qualitative variations in behavior between lipid samples were consistent for all samples. The fraction helix results presented herein are for typical samples.

Circular Dichroism. Far-UV CD spectra were measured on a J-810 spectrometer (Jasco, Easton, MD) using a 1 mm quartz cell. The protein concentration was 0.25 mg/mL, unless stated otherwise, while lipid concentrations varied from 0 to 10 mM. Typically, a scanning rate of 50 nm/min and a bandwidth of 0.5 nm with a time response of 2 s were used to obtain CD spectra as an average of four scans. The final spectra were obtained by subtracting a background spectrum obtained on just micelles or vesicles without protein in the same cell. Unless specifically stated otherwise, all spectra were recorded above the lipid phase transition, i.e., in the liquid crystalline phase, using a thermostated cell holder. This can particularly impact the DSPG results relative to the others, due to its higher-temperature phase transition. The temperature dependence of the βLG−lipid complex CD was determined by measuring complete spectral scans every 5 °C from 5 to 90 °C with automated control of the sample temperature via a circulating (Neslab RT-7) bath. The fractional secondary structure for βLG in the absence and presence of lipid micelles or vesicles was estimated from the CD spectra by use of the SELCON 3 program of the CDPro software package (*16*), whereas due to spectral interference, the helical contents were estimated using just the ellipticity at 222 nm for urea denaturation experiments (*17*).

Fluorescence Measurements. Fluorescence measurements were performed on a Fluoromax-3 (Jobin Yvon Inc., Edison, NJ) spectrofluorometer. The excitation wavelength was 295 nm, and the emission was scanned from 300 to 450 nm. In all experiments, background spectra, either of the buffer alone or of the buffer containing vesicles, were subtracted from the corresponding sample spectra. The concentration of βLG for all fluorescence measurements was kept at ∼0.25 mg/mL.

For fluorescence anisotropy experiments, the excitation and emission wavelengths were 360 and 425 nm, respectively, when DPH or TMA-DPH was being observed. Fluorescence anisotropies were determined using standard procedures (taken from the J-Y operation manual), according to the equation $r = I_{VV} - GI_{VH}/I_{VV} + 2GI_{VH}$, where I_{VV} and I_{VH} are the intensities observed with vertical (V) or horizontal (H) orientations of the excitation and emission polarizers, while I_{HV} and I_{HH} are the same fluorescence intensities measured with the excitation light horizontally polarized. G is the (grating) correction factor given by $G = I_{HV}/I_{HH}$, determined by measuring the polarized fluorescence of the protein or probes with horizontally polarized excitation.

For fluorescence experiments designed to model fatty acid transport, βLG was incubated with 2-(9-anthroyloxy)stearic acid at room temperature for 10 min, and the resulting complex was incubated with DMPG vesicles for 30 min at room temperature. The emission fluorescence in the region of 380−650 nm was recorded at the excitation wavelength of 360 nm using emission and excitation slits of 5 nm. Because this fluorescent fatty acid analogue partitions into phospholipid vesicles to give an increase in fluorescence intensity, titrations involving addition of phospholipid vesicles to a highly fluorescent βLG−analogue system were corrected by performing the titration in the absence of βLG as a control.

ATR-FTIR Measurements. Fourier transform infrared (FTIR) absorbance measurements were performed as previously described (*14*, *18*, *19*). Briefly, polarized attenuated total reflectance (ATR)-FTIR experiments were conducted on a Digilab FTS60A (Varian, Randolf, MA) spectrometer equipped with a MIRacle ATR accessory (PIKE Technologies, Inc., Madison, WI), incorporating a three-reflection ZnSe ATR Universal Plate. Approximately 10 μL of sample solution containing lipid vesicles with βLG was pipetted onto the recessed plate and then dried under a gentle stream of nitrogen gas to form a thin film on the surface of the ZnSe plate. This process was repeated until enough sample built up and the absorbance did not change. Polarization spectra were recorded for 0° and 90° orientations of a wire grid polarizer placed in front of the sample. The dichroic spectra were obtained by subtracting a spectrum recorded with parallel (||) polarized light from that recorded with perpendicular ($\perp$) polarized light, using a weight coefficient, R_{iso}, defined as the ratio of integrated absorbance of the lipid carbonyl band at ~1740 cm^{-1} in spectra measured with || polarization of the incident light to that with $\perp$ polarization (*20*, *21*). Protein amide I transition differential polarizations are then referenced to the results for the lipid aliphatic CH_2 scissor and wag modes to establish the relative orientations of helices and sheets to the hydrocarbon chains and thus to the membrane surface.

Monolayer Measurements. Monolayer measurements were performed as described elsewhere (*22*). Briefly, the surface pressure (π) of a solution in a circular Teflon trough (4 cm diameter × 1 cm deep) was measured using a Wilhelmy plate attached to a computer-controlled Cahn microbalance. The lipid monolayers were spread from a phospholipid solution in a chloroform/methanol mixture (3:1, v/v) onto 10 mL of a subphase (10 mM PBS) under continuous stirring with a magnetic bar to give an initial surface pressure (π_0). Once the increase in surface pressure for the monolayer had stabilized (after 5−10 min), the βLG was injected into the subphase through a hole in the edge of the trough, and the change in surface pressure ($\Delta\pi$) was measured as a function of time. Typically, the $\Delta\pi$ value reached a maximum in ~20 min. The maximum $\Delta\pi$ at a given π depended on the protein concentration and reached a saturation value when the protein concentration was above a certain value. Protein concentrations in the subphase were maintained above this value to ensure that the observed $\Delta\pi$ represented a maximum value. The critical surface pressure (π_c), defined as the maximal surface pressure allowing a protein insertion, was determined by extrapolating the $\Delta\pi$ versus π_0 plot to its *x*-axis intercept.

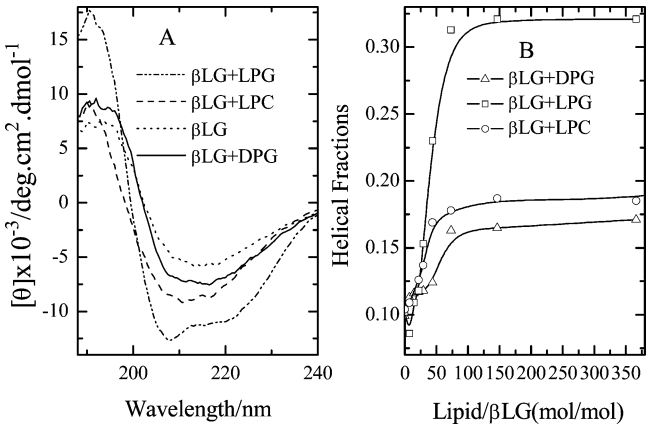

FIGURE 1: Micelle-induced conformational transition in 0.25 mg/mL βLG. (A) Far-UV CD spectra of βLG (•••) and βLG in the presence of 2 mM DPG (—), LPC (- - -), and LPG micelles (-•-). (B) Helical fraction changes as a function of lipid:protein ratio for DPG (△), LPC (○), and LPG (□).

RESULTS

Conformational Transition in βLG Induced by Different Lipid Vesicles and Micelles. To examine the role of hydrophobic interaction in membrane binding of βLG, neutral LPC (C-14, single chain) and negatively charged (LPG, C-14, single chain, and DPG, C-8, double chains) micelles as well as anionic phospholipid vesicles (with various hydrocarbon chains) were used in this work. As shown in Figure 1A, in the native state, βLG exhibits a typical β-sheet dominant far-UV CD spectrum with a wide minimum around 216 nm (•••). With the addition of 2 mM neutral micelles of LPC (- - -) and negatively charged micelles of DPG (—) and of LPG (-•-) at pH 6.8, βLG exhibited an increase in ellipticity at 222 nm. This feature, which is consistent with a small increase in the level of α-helical structure, is most significant for βLG and LPG. Average secondary structure variation determined using CDPro (*16*) corresponds to an increase in the apparent level of α-helical structure from 10% in the native state to ~20, ~18, and ~32% in the presence of LPC (○), DPG (△), and LPG (□) micelles, respectively, as shown in Figure 1B. It should be noted that the neutral micelles of LPC induced a small increase in helical structure content, whereas neutral lipid vesicles of DMPC alone (not shown) did not induce any significant conformational transition in βLG (*12*, *14*). The LPC-induced increase in the level of α-helical structure is more pronounced at pH 6.8, instead of pH 4.6 (data not shown), suggesting that the βLG−LPC interaction is hydrophobic in nature. Similar behavior has been observed for apocytochrome *c*, which in neutral LPC micelles attains ~65% of the helix content of the native state in solution, while in zwitterionic phospholipid vesicles, apo-cyt *c* is unable to fold (*23*). Negative detergent micelles induce even higher helicity in cytochrome *c* (*18*, *24*). In the case of DPG micelles (C-8), despite having a negatively charged head group, only a small added fraction of α-helix was induced, indicating again that the electrostatic interaction alone is not enough to induce a substantial β-to-α transition. By contrast, LPG micelles (C-12) induced a relatively strong β-to-α transition in βLG. Since both micelles have negative head groups, but different tail lengths, this observation further demonstrates that in addition to an electrostatic

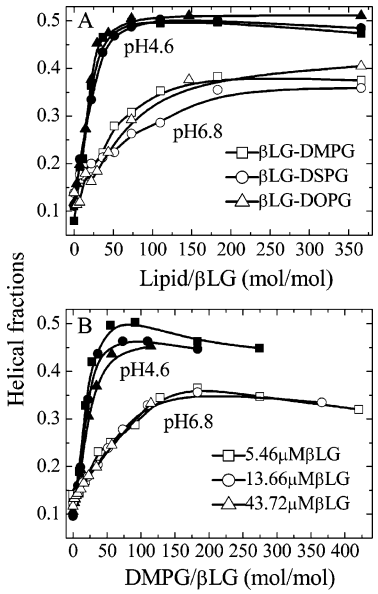

FIGURE 2: Lipid:βLG ratio-dependent induced helical fractions followed by far-UV CD. (A) βLG interacting with different lipid vesicles, DMPG (□ and ■), DSPG (○ and ●), and DOPG (△ and ▲) at pH 6.8 (open symbols) and pH 4.6 (black symbols). (B) Different concentrations of βLG interacting with DMPG. Squares, circles, and triangles depict data for 5.46, 13.66, and 43.72 μM βLG, respectively, at pH 6.8 (open symbols) and pH 4.6 (black symbols). All spectra were measured in the liquid crystalline phase.

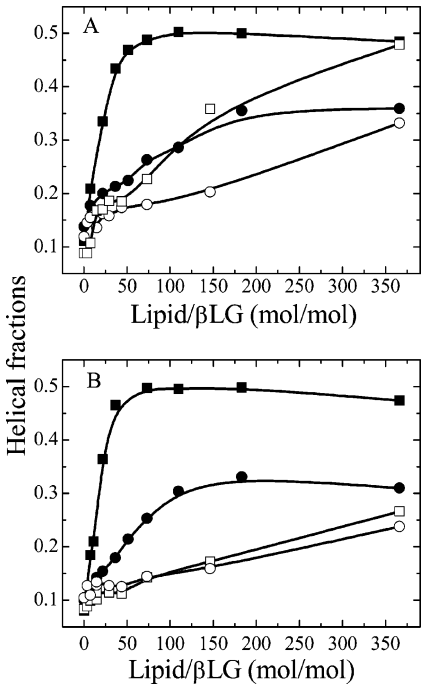

FIGURE 3: Effect of lipid packing on the β-to-α transition in βLG. (A) Helical fractions induced by DSPG in the gel (open symbols) and liquid crystalline (black symbols) states at pH 6.8 (○ and ●) and pH 4.6 (□ and ■). (B) Helical fractions induced by DMPG (black symbols) and DMPA (open symbols) at pH 6.8 (○ and ●) and pH 4.6 (□ and ■), respectively, followed by far-UV CD. α-Helical fractions were estimated using the Selcon part of the CDPro program.

driving force (*14*), hydrophobic interaction between phospholipids and βLG is required for the development of the conformational transition.

To study the role of hydrophobic interaction further, interactions of βLG with vesicle-forming lipids having the same head group but different acyl chains were studied. As shown in Figure 2A, the induced helical contents for βLG with DMPG (C-12), DSPG (C-18), and DOPG (C-18, one double bond) follow virtually the same lipid concentration-dependent traces and reach a plateau when the lipid:protein molar ratio is above ~70 at pH 4.6 and above ~150 at pH 6.8. The magnitudes of the helical fraction did vary; however, for identically prepared samples, the spectra overlapped, and for various conditions, the concentration trends were consistent. For these data, all samples were adjusted in temperature so that the lipid was in the liquid crystalline state regardless of their hydrocarbon nature, which leads to the overlap since the degree of helicity induced is temperature-dependent (*14*), as discussed further below. This observation indicates that the phospholipid-induced helical contents strongly depend on the lipid:protein ratio; i.e., at each pH value, the βLG interacts with all these tested lipids to form helical fractions at almost the same stoichiometry. At lower pH, achieving the maximum value of helix content requires a lower lipid:protein ratio compared to that at higher pH. The length and saturation character of the lipid chains appear to have only a minor effect on vesicle binding of βLG, given comparable phase conditions, unless the hydrocarbon chains of the phospholipids are too short. We assume that for DPG, the hydrophobic interactions between βLG and the short carbon chains are not as effective in maintaining the helix fraction. The helical content induced by DSPG is somewhat smaller than that induced by other lipid vesicles at pH 6.8 (Figure 2A), which may be due to recording spectra at 65 °C (above the DSPG melting point, ~55 °C), conditions under which the protein may partially unfold (*14*). Additionally, for βLG at different concentrations (with DMPG), the helical fractions come to a maximum (Figure 2B) at the same lipid:βLG ratio and reach almost the same helical content as in Figure 2A at both pH 4.6 and 6.8.

The lipid packing property also has an effect on the βLG β-to-α transition. As seen in Figure 3A, the interaction of βLG with DSPG in the gel state (room temperature) follows a different trace than for the liquid crystalline state (~63 °C). In the gel state (□ and ○ for pH 4.6 and 6.8, respectively), the increase in helical content is much less sensitive to an increase of DSPG concentration than that seen for the liquid crystalline state (■ and ● for pH 4.6 and 6.8, respectively). However, the maximum/final α-helical content we obtained is almost the same for βLG with DSPG in both the gel and liquid crystalline states; it is just that the required amount of lipid differs (in terms of the lipid:protein ratio).

To further study the effect of lipid packing on the β-to-α transition in βLG, two lipids (DMPG and DMPA) with the same acyl chains but different negatively charged head groups, which result in different lipid packing properties, were used. In comparison with DMPG, DMPA has a higher packing density, as evidenced by its higher phase transition temperature. As shown in Figure 3B, DMPA in the gel state can induce only a small degree of α-helix formation in βLG (□ and ○ for pH 4.6 and 6.8, respectively), resulting in a gradual transition, while by contrast, a small amount of DMPG can induce a stronger $\beta \rightarrow \alpha$ transition (■ and ● for pH 4.6 and 6.8, respectively). Collectively, these observations indicate that lipid packing has a significant effect on protein−lipid interaction, under the conditions of the same net charge

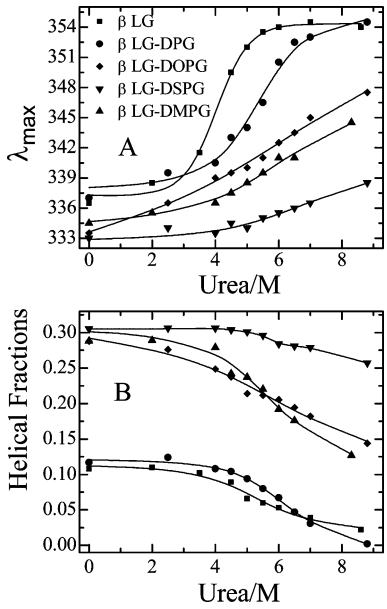

FIGURE 4: Stability of the lipid−βLG complex against urea followed by intrinsic fluorescence (A, λ_{max}) and by far-UV CD (B, helical fraction vs. urea) at pH 6.8 (13.66 μM βLG and 1.5 mM lipids). Squares, circles, diamonds, triangles, and inverted triangles depict data for βLG alone and βLG complexed with PG, DOPG, DMPG, and DSPG, respectively. α-Helical fractions were estimated from ellipticity at 222 nm in far-UV CD spectra according to ref *17*.

and/or the same hydrocarbon chain lengths for the phospholipids.

Stability of Lipid-Bound βLG. Above, we showed that βLG undergoes a clear β-to-α transition in the presence of anionic phospholipid micelles and vesicles (except DPG). Figure 4 summarizes two measures of the degree of denaturation of βLG−lipid complexes induced by addition of urea. Loss of βLG tertiary structure, as evidenced by the shift in λ_{max} for the intrinsic fluorescence, is monitored in Figure 4A, and the loss of α-helical fractional secondary structure, as derived from CDPro analysis of far-UV CD, is monitored in Figure 4B. The secondary and tertiary transitions are in qualitative agreement in terms of relative stability with respect to urea in different lipids but differ in detail.

Forming a lipid−βLG complex in general leads to a stabilization of the tertiary structure from urea denaturation (higher C_m) and some stability for the induced helix. With denaturation by urea, the βLG−DPG complex exhibits tertiary structure stability [C_m = 5.3 M (●)] higher than that of βLG alone [C_m = 4.03 M (■)] as followed by λ_{max} (Figure 4A). In both cases, λ_{max} shifted from 337 to 355 nm with an increase in urea concentration, a value characteristic of totally exposed Trp residues. On the other hand, with no urea, there is a clear blue shift in the λ_{max} of βLG in the presence of DMPG (▲), DOPG (◆), and DSPG (▼), which is consistent with βLG membrane insertion. As compared with the stability of βLG alone or in DPG micelles, these βLG−lipid vesicle complexes show stronger resistance to loss of tertiary structure, or at minimum chromophore solvation, under urea denaturation. While the λ_{max} increased with an increase in urea concentration for βLG in lipid vesicles, it did not attain a value indicating solvent-exposed Trp residues, even at 8 M urea, a condition under which βLG alone would be totally unfolded [Figure 4A (■)], resulting in the Trp being fully exposed to polar solvents. Shielding of Trp versus the lipid type also correlates with the stability of secondary structure as can be seen by comparing the smaller variation in λ_{max} for βLG in DSPG, as compared to DMPG and DOPG (Figure 4A), and similarly smaller decrease in helix content (Figure 4B; see below), i.e., indicating more protection from urea unfolding.

The stability of the βLG−lipid complex secondary structure was studied by estimating changes in α-helical contents from far-UV CD as a function of urea concentration. As shown in Figure 4B, for native βLG (■) or βLG-DPG (●), an increase in the urea concentration reduces the α-helical content of βLG to virtually zero, suggesting full unfolding of βLG alone or in the presence of DPG micelles. By contrast, the helical contents of βLG in the presence of DMPG (▲), DOPG (◆), and DSPG (▼) vesicles decreased with an increase in urea concentration but preserve much more α-helical structure than for unfolded βLG. This phenomenon is most pronounced for βLG in the presence of DSPG, where βLG still retains ∼26% helical structure even at 8.8 M urea. The fluorescence results suggest that βLG penetrates into the DMPG, DSPG, and DOPG vesicle lipid bilayers. Consequently, the βLG helical segments could be shielded from urea, thus stabilizing them against unfolding, which is consistent with the CD results.

In parallel with the urea denaturation results, we have previously shown by external fluorescence quenching (*14*) that βLG penetrates DMPG membranes. Acrylamide titrations of βLG in DOPG and DSPG vesicles yielded quenching plots (data not shown) with slopes similar to those of the native protein titrations, indicating all three vesicles provide significant protection for the Trp residues against quenching with acrylamide.

By contrast to the fairly well delineated conformational transitions in Figure 4, as induced by addition of urea, the temperature dependence of the protein−lipid vesicle complexes showed little evidence of a cooperative phase transition. The CD of 250:1 and/or 125:1 lipid/βLG samples was monitored from 5 to 90 °C for DMPG, DOPG, and DSPG vesicles at pH 6.8 and 4.6 (data not shown). The resulting variations were monotonic but lacked a clear transition, much as previously reported (*14*).

Membrane Penetration of βLG. To gain more insight into the balance of hydrophobic and electrostatic interactions driving βLG−membrane penetration, we monitored the effects of penetration of βLG into various lipid monolayers at the air−water interface. The phospholipid monolayer was spread to a constant area, and the change in surface pressure ($\Delta\pi$) for various initial pressures (π_0) was monitored after injection of the protein into the subphase. In general, $\Delta\pi$ is inversely proportional to π_0 of the monolayer, and extrapolation of the $\Delta\pi$ versus π_0 plot yields the critical surface pressure (π_c), which specifies the upper limit of a monolayer π_0 into which a protein can penetrate, or the lipid monolayer surface pressure needed to exclude the protein (*22*). Thus, for different lipids, the higher the π_c, the more easily the protein can penetrate the monolayer. Our recent study demonstrated that zwitterionic lipid vesicles (DMPC) are unable to induce a clear β-to-α transition in βLG; therefore, DMPC monolayers were used as controls in this experiment. As shown in Figure 5A, at pH 6.8 the weak interaction of βLG with DMPC yields a π_c of ∼22.4 dyn/cm (□), whereas

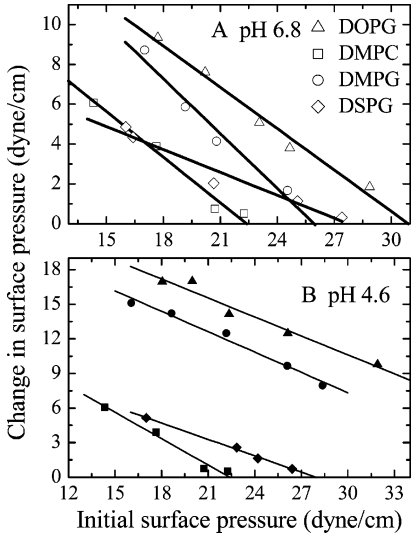

FIGURE 5: Monolayer penetration of βLG. Change in the surface pressure at different initial pressures resulting from a saturating concentration (25 μg/mL) of βLG interacting with DMPC (□ and ■) as a reference state for insertion of βLG into DOPG (▲ and △), DMPG (○ and ●), and DSPG (◇ and ◆) monolayers at pH 6.8 (A, open symbols) and pH 4.6 (B, black symbols).

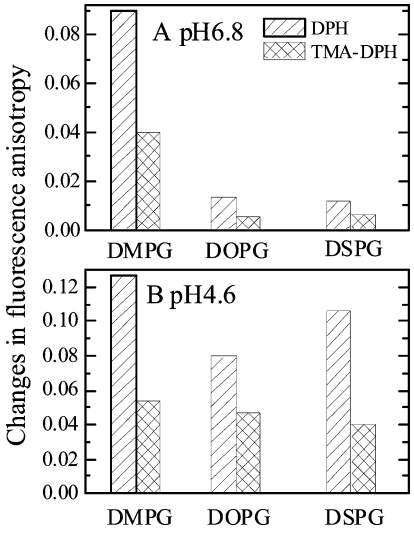

FIGURE 6: Fluorescence anisotropy changes after the addition of βLG into phospholipid bilayers. βLG (50 μM) was incubated with 1.0 mM DOPG, DMPG, and DSPG vesicles containing DPH and TMA-DPH at pH 6.8 (A) and pH 4.6 (B), respectively. The fluorescence anisotropy was recorded above the transition temperature of tested lipids, and the fluorescence anisotropy changes were obtained from the subtraction of the fluorescence anisotropy for free lipid vesicles from that for βLG−lipid complexes. Bar heights represent the average of 30 measurements for each sample.

π_c is significantly higher for monolayers of DMPG [$\pi_c \approx$ 26.8 dyn/cm (○)], DSPG [$\pi_c \approx$ 27.9 dyn/cm (◇)], and DOPG [$\pi_c \approx$ 30.9 dyn/cm (△)], indicative of some penetration of βLG into these anionic lipid monolayers. Compared to those of DSPG and DMPG, the higher π_c value for DOPG implies βLG can more deeply penetrate the monolayer. This indicates that, for the lipids with the same head group, the lipid packing has a significant effect on insertion of protein into the membrane, i.e., the tighter the phospholipid packing, here correlated to the phase transition temperature, the less the protein inserts. These examples have the same head group but differ in lipid phase stability due to their acyl chain length and composition, DOPG being the most fluid (lowest phase transition).

The π_c values at pH 4.6 (Figure 5B) are higher than those at pH 6.8, which is consistent with the increased membrane penetration at pH 4.6 versus that at pH 6.8, as seen above for vesicles. The unusual slope of the DSPG result subjects determination of its π_0 to more error and may indicate effects of lipid packing properties due to it being in a state different from that of the other lipids under these experimental conditions. (The monolayer experiments were constrained to room temperature at which DSPG is in a gel state, while DOPG is in a fluid state, and DMPG is near its transition temperature.) The higher π_c values at a lower pH value may result from the strong electrostatic interactions of βLG with anionic lipids at pH 4.6, causing more hydrophobic residues to be exposed, which in turn yields more penetration of βLG into membrane.

The effect of protein insertion on the phospholipid membrane structural properties was further investigated by measuring the steady-state fluorescence anisotropy of the fluorescent probes, DPH and TMA-DPH, incorporated into lipid vesicles as a function of protein concentration. DPH and TMA-DPH are useful for the study of the phospholipid bilayer structural order. Whereas DPH is thought to be fully inserted into the lipid bilayers with its longitudinal axes parallel to the acyl chains, TMA-DPH is constrained to be near the interfacial region, due to the trimethylammonium cation group (*25*), with its fluorophore extending parallel to the fatty acyl chains approximately to the level of the eighth to tenth carbon. The absorption and emission moments of DPH are almost parallel and aligned to its longitudinal axis (*25*). Figure 6 shows changes in fluorescence anisotropy of DPH and TMA-DPH probes caused by the addition of 50 μM βLG at pH 6.8 and 4.6, respectively, to DMPG, DOPG, and DSPG lipid vesicles. βLG has a greater effect on the DPH anisotropy than on the TMA-DPH anisotropy for all vesicles, but the effect is most dramatic for DMPG generally and is larger for the others at low pH. βLG binding appears to have a more pronounced effect on the environment of DPH in the hydrophobic interior than when it is constrained to be close to the membrane interface, consistent with insertion of the peptide chain into the bilayer. While a similar ratio is observed for DOPG and DSPG quantitatively, at pH 6.8 βLG has only a minor effect on both the DPH and TMA-DPH anisotropy of DOPG and DSPG vesicles, implying less disruption of the hydrophobic interior of the vesicle bilayer. At pH 4.6, βLG caused considerably more change in DPH and TMA-DPH anisotropy for all three vesicle systems as compared with those at pH 6.8, indicative of stronger perturbation of the membrane structure at lower pH, which is consistent with the observations above suggesting greater penetration of βLG into the membrane at a lower pH value.

Protein Orientation in the Lipid Bilayer and FTIR-ATR Results. The polarized FTIR-ATR spectra of βLG in DSPG lipid bilayers (Figure 7) behaved in a manner similar to that of our previously reported (*14*) results for DMPG. Despite the poor resolution of contributions to amide I, which is typical of globular proteins, the helical component (~1650 cm^{-1}) is clearly positive, opposite in sign to the CH_2 scissor mode, and thus, the amide C═O groups are oriented preferentially perpendicular to the membrane surface (parallel

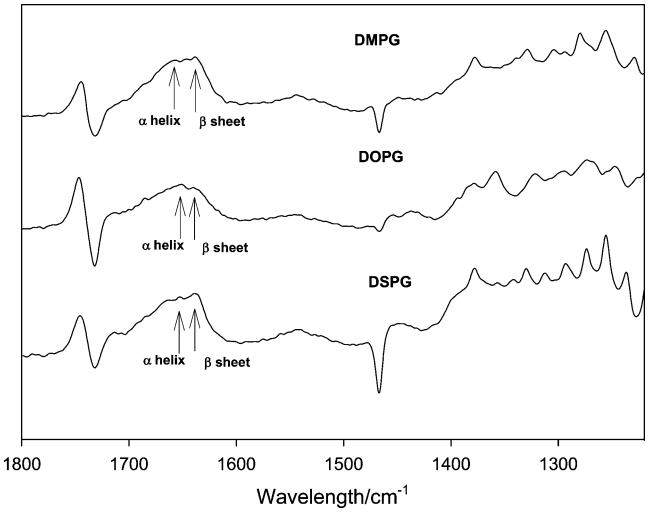

FIGURE 7: Polarized ATR-FTIR difference spectra (90°−0° polarization) of DMPG, DOPG, and DSPG (from top to bottom, 250:1 lipid:protein ratio) at pH 6.8. For clarity, the spectra are offset.

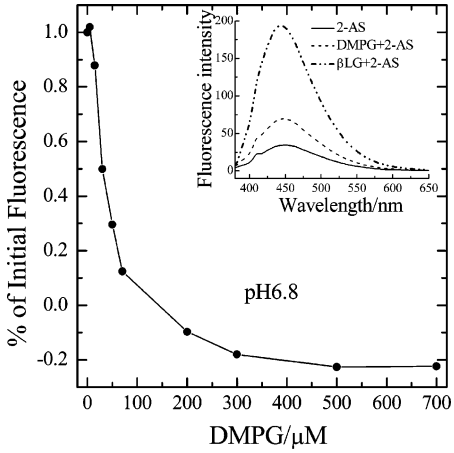

FIGURE 8: Evidence of the transportation of 2-AS fatty acid by βLG via the interaction with DMPG as demonstrated by a loss of fluorescence (●) of the βLG−2-AS complex on binding lipid vesicles at pH 6.8. The inset shows fluorescence spectra of 2-AS (—), the βLG−2-AS complex (-···-), and a DMPG/2-AS mixture (- - -).

to the relatively well ordered acyl chains), which suggests helical insertion into the bilayer (C═O mostly parallel to the helix axis). The sheet component (∼1630 cm^{-1}) has the same sign, but since its C═O modes would be perpendicular to the β-strands, it is most likely that these strands are preferentially parallel to the surface, and probably on it, although this is clearly more difficult to conclude from the data. The βLG in DOPG results imply a less well defined protein helical orientation (and almost no sheet), which seems to result from the DOPG lipid structure being clearly less ordered, which is evident from the weak dichroism of the CH_2 scissor and wag bands (∼1450 and 1300 cm^{-1}). Both DMPG and DOPG were in the liquid crystalline phase, while DSPG was in the gel state for these ATR experiments. The DSPG results showed more order (evidenced as more dichroism for both lipid and protein components) but were somewhat sensitive to the sample preparation, whether the protein was added above or below the phase transition temperature. However, if the water was thoroughly removed by drying the film, the end results were consistent.

Transfer of Fatty Acids. In spite of the number of studies on βLG, its physiological function still remains unclear. Since βLG has a structure quite similar to that of fatty acid binding proteins and retinal binding proteins, which form a conical central calyx or cavity to provide a binding site for hydrophobic ligands, it has been proposed that βLG could have a retinal or fatty acid transport role (*5*). In this study, 2-AS was used as a fluorescent fatty acid analogue to probe the possibility of transport of fatty acid from βLG to membranes. As shown in the inset of Figure 8, binding of 2-AS to βLG results in a considerable fluorescence enhancement (-···-), consistent with 2-AS being located in an apolar environment within βLG. In contrast, there is a much smaller increase in fluorescence when 2-AS partitions into just a membrane (- - -) as compared with that of free 2-AS (—). The percentage fluorescence change [plotted as $\Delta F/F \times 100\%$, where ΔF is the decrease in fluorescence and F is the fluorescence of the lipid-free βLG−2-AS complex, as described elsewhere (*26*)] observed upon addition of DMPG vesicles reflects the induced release of 2-AS from βLG. As seen from Figure 8, the fluorescence of 2-AS complexed with βLG decreases sharply with added DMPG vesicles. This behavior is consistent with addition of lipid vesicles causing the fluorophore to be released from the protein, much as a fatty acid would be released at a receptor. The $\Delta F/F$ values for βLG-bound 2-AS (pH 6.8) reach a roughly constant level for addition of >300 μM DMPG. However, these values become negative, which may be due to the change in the environment for the mixed protein−lipid state or to error in correcting for background (2-AS in DMPG) in these low-level fluorescence signals.

DISCUSSION

Governing Force for the Lipid-Induced Conformational Transition in βLG. The transition of proteins from solution to the membrane-associated state involves a number of steps: initial binding to the surface, induction or stabilization of a specific lipid-bound secondary structure, modulation of membrane biophysical properties by protein binding, and finally either partial or full insertion of the protein into the membrane (*27*, *28*). In these processes, the protein structure may undergo dramatic changes, including a disruption of tertiary structure and/or a formation of specific lipid-bound secondary structure, concomitant with a change in the lipid physical state. Generally, it has been established that electrostatic interactions between polar residues of the protein and negatively charged phospholipids are the dominant forces which direct adsorption of the protein onto the membrane surface. Nonpolar interactions between apolar segments of the protein and the lipid hydrophobic chains lead to insertion of the protein into the membrane interface, which in turn results in a disruption of the membrane structure.

Previous studies and our own recent work on the interaction of βLG with lipids demonstrate that zwitterionic phospholipid vesicles do not cause a significant conformational transition, whereas anionic phospholipid vesicles induce a dramatic β-to-α transition in βLG (*12*−*14*). This is enhanced by lowering the pH since, with a pI of 5.3, βLG changes from a net negative charge at pH 6.8 to a net positive charge at pH 4.6. These results led to a conclusion that the binding of βLG to negatively charged lipids is driven by electrostatic effects, since it is reduced with an increased ionic strength and susceptible to pH titration and a change

in lipid charge, whereas the hydrophobic interaction appeared to play a minor role. Previous studies on the interaction of βLG with alcohols demonstrated that the ability to induce the β-to-α transition in βLG improves with the hydrophobic character of the denaturant alcohol and has been further confirmed by the study of different colloidal media (*8*, *29*).

The ability of zwitterionic lysophospholipids to induce a substantial conformational transition in βLG reveals that the interaction between βLG and lipids can have different mechanisms. This micellar interaction (in contrast to our vesicle results) may be a hydrophobic property, much like the interaction of detergents with proteins, such as we have previously studied with cytochrome *c* (*18*), and may be influenced by the added curvature of the micelles. Nonetheless, for βLG, electrostatic interaction is still a dominant component since the higher degree of β-to-α transition can be achieved only by negatively charged lipid vesicles or micelles. The sharply reduced ability of the negatively charged phospholipid with short hydrocarbon chains (DPG, C-8) to induce a β-to-α transition in βLG, together with the minimal effect of pure salt, further demonstrates that hydrophobic interaction is indispensable for these lipid-induced conformational changes; i.e., the electrostatic interaction alone is not sufficient for unfolding and significantly stabilizing helical βLG. It should be emphasized that, in the absence of either electrostatic or hydrophobic interactions, the conformational transition is weakened, and only when both interactions are present can the highest degree of the transition be achieved.

By comparing the helical content induced by DPG with that induced by other phospholipids with the same headgroup, we find that hydrophobic interaction may further extend or stabilize the lipid-bound βLG structure, through the membrane insertion as can be inferred from a combination of observations, as noted below. The mechanism is deduced to be a combination of electrostatic interactions initiating the membrane binding process, presumably leading to protein unfolding, and then partial insertion limited by lipid packing characteristics which results in the final protein vesicle stability and degree of helix induction.

Governing Force for the Penetration of βLG into Phospholipid Bilayers. Once bound onto the membrane surface, the next question about protein−membrane structure is what chemical and structural factors control penetration of protein into membranes. It is generally recognized that proteins destined to cross membranes need to maintain an unfolded or loose conformation. This observation has been confirmed in the previous studies of the interaction of α-lactalbumin with phospholipid membranes (*30*, *31*).

In the case of βLG, Brown et al. (*32*) found that when the α-helix content was increased to some extent, zwitterionic phopholipids were able to bind to the protein, which was not possible for the native form of βLG. Previous studies of the interaction of βLG with phospholipids at an air−liquid interface showed that the role of the hydrophobic interaction might be linked to the changes in conformation during the adsorption process, which can facilitate the insertion of βLG into phospholipid monolayers (*33*, *34*). They concluded that not only electrostatic but also hydrophobic interactions are important for the incorporation of βLG into phospholipid monolayers. However, a previous FTIR study showed that βLG−lipid interactions are independent of the lipid chain length and the behavior of βLG could be seen to be consistent with an extrinsic protein mainly bound to the membrane surface by electrostatic interactions (*12*, *13*).

In contrast, our studies demonstrate that a portion of βLG is inserted into the vesicle bilayers, as evidenced by the blue shift in the fluorescence λ_{max}, by an only small increase in the level of acrylamide quenching and by the βLG helical orientation as detected by the polarized ATR-IR studies (Figure 7) (*14*). The same behavior is evident in DMPG, DOPG, and DSPG bilayers, albeit with variations reflecting the packing properties of each lipid system. The urea stability (Figure 4) and monolayer surface pressure measurements (Figure 5) further support the model of insertion of the protein into the lipid layer and bring out a dependence on chain length and lipid packing density that suggests charge alone is not sufficient for the formation of a stable protein−membrane complex. Our results suggest an initial partial unfolding of the tertiary structure on the surface, promoted by charge interaction, is a prerequisite for penetration of βLG into membranes. While the hydrophobic potential of the lipids alone is not sufficient to stabilize the helical structure, they can play a significant role in the insertion and stabilization of the protein−membrane complex.

This model also explains the fatty acid (2-AS) transport tests we devised to model biomolecular function. Upon interacting with the membrane, the βLG−2AS complex releases 2-AS to the vesicle, which is consistent with the protein unfolding on the membrane surface due to charge interaction before its partial insertion. The role of βLG as a transporter that can yield its ligand to a receptor on the membrane surface is seen to be reasonable.

ACKNOWLEDGMENT

We thank Prof. Wonhwa Cho for access and Dr. Robert Stahelin for help with measurement and discussion of the membrane monolayer experiment.

REFERENCES

1. Nussbaum, R. L., and Ellis, C. E. (2006) Alzheimer's disease and Parkinson's disease, *N. Engl. J. Med. 348*, 1356−1364.
2. Careel, R. W., and Lomas, D. A. (1997) Conformational disease, *Lancet 350*, 134−138.
3. Hirsh, D. J., Hammer, J., Maloy, W. L., Blazyk, J., and Schaefer, J. (1996) Secondary structure and location of a magainin analogue in synthetic phospholipid bilayers, *Biochemistry 35*, 12733−12741.
4. Killian, J. A. (1998) Hydrophobic mismatch between proteins and lipids in membranes, *Biochim. Biophys. Acta 1376*, 401−416.
5. Sawyer, L., and Kontopidis, G. (2000) The core lipocalin, bovine β-lactoglobulin, *Biochim. Biophys. Acta 1482*, 136−148.
6. Qin, B. Y., Creamer, L. K., Baker, E. N., and Jameson, G. B. (1998) 12-Bromododecanoic acid binds inside the calyx of bovine β-lactoglobulin, *FEBS Lett. 438*, 272−278.
7. Wu, S., Pérez, M. D., Puyol, P., and Sawyer, L. (1999) β-Lactoglobulin binds palmitate within its central cavity, *J. Biol. Chem. 274*, 170−174.
8. Hirota, N., Mizuno, K., and Goto, Y. (1997) Cooperative α-helix formation of β-lactoglobulin and melittin induced by hexafluoroisopropanol, *Protein Sci. 6*, 416−421.
9. Mendieta, J., Folqué, H., and Tauler, R. (1999) Two-phase induction of the nonnative α-helical form of β-lactoglobulin in the presence of trifluoroethanol, *Biophys. J. 76*, 451−457.
10. Beringhelli, T., Eberini, I., Galliano, M., Pedoto, A., Perduca, M., Sportiello, A., Fontana, E., Monaco, H. L., and Gianazza, E. (2002) pH and ionic strength dependence of protein (un)folding and ligand binding to bovine β-lactoglobulins A and B, *Biochemistry 41*, 15415−15422.

11. Viseu, M. I., Carvalho, T. I., and Costa, S. M. B. (2004) Conformational transitions in β-lactoglobulin induced by cationic amphiphiles: Equilibrium studies, *Biophys. J. 86*, 2392−2402.
12. Lefevre, T., and Subirade, M. (2000) Interaction of β-lactoglobulin with phospholipid bilayers: A molecular level elucidation as revealed by infrared spectroscopy, *Int. J. Biol. Macromol. 28*, 59−67.
13. Lefevre, T., and Subirade, M. (2001) Conformational rearrangement of β-lactoglobulin upon interaction with an anionic membrane, *Biochim. Biophys. Acta 1549*, 37−50.
14. Zhang, X., and Keiderling, T. A. (2006) Lipid-induced conformational transitions of β-lactoglobulin, *Biochemistry 45*, 8444−8452.
15. Rankin, S. E., Watts, A., Roder, H., and Pinheiro, J. T. (1999) Folding of apocytochrome c induced by the interaction with negatively charged lipid micelles proceeds via a collapsed intermediate state, *Protein Sci. 8*, 381−393.
16. Sreerama, N., and Woody, R. W. (2000) Estimation of protein secondary structure from circular dichroism spectra: Comparison of CONTIN, SELCON, and CDSSTR methods with an expanded reference set, *Anal. Biochem. 287*, 252−260.
17. Chen, Y. H., Yang, J. T., and Chau, K. H. (1974) Determination of the helix and β form of proteins in aqueous solution by circular dichroism, *Biochemistry 13*, 3350−3359.
18. Xu, Q., and Keiderling, T. A. (2004) Effect of sodium dodecyl sulfate on folding and thermal stability of acid-denatured cytochrome c: A spectroscopic approach, *Protein Sci. 13*, 2949−2959.
19. Xu, Q., and Keiderling, T. A. (2005) Trifluoroethanol-induced unfolding of concanavalin A: Equilibrium and time-resolved optical spectroscopic studies, *Biochemistry 44*, 7976−7987.
20. Goormaghtigh, E., Raussens, V., and Ruysschaert, J. M. (1999) Attenuated total reflection infrared spectroscopy of proteins and lipids in biological membranes, *Biochim. Biophys. Acta 1422*, 105−185.
21. Tatulian, S. A. (2003) Attenuated total reflection Fourier transform infrared spectroscopy: A method of choice for studying membrane proteins and lipids, *Biochemistry 42*, 11898−11907.
22. Stahelin, R. V., Long, F., Diraviyam, K., Bruzik, K. S., Murray, D., and Cho, W. (2002) Phosphatidylinositol 3-phosphate induces the membrane penetration of the FYVE domains of Vps27p and Hrs, *J. Biol. Chem. 277*, 26379−26388.
23. Bryson, E. A., Rankin, S. E., Goormaghtigh, E., Ruysschaert, J. M., Watts, A., and Pinheiro, T. J. T. (2000) Structure and dynamics of lipid-associated states of apocytochrome c, *Eur. J. Biochem. 267*, 1390−1396.
24. Rankin, S. E., Watts, A., and Pinheiro, T. J. T. (1998) Electrostatic and hydrophobic contributions to the folding mechanism of apocytochrome c driven by the interaction with lipid, *Biochemistry 37*, 12588−12595.
25. Kaiser, R. D., and London, E. (1998) Location of Diphenylhexatriene (DPH) and Its Derivatives within Membranes: Comparison of Different Fluorescence Quenching Analyses of Membrane Depth, *Biochemistry 37*, 8180−8190.
26. Davies, J. K., Thumser, A. E. A., and Wilton, D. C. (1999) Binding of Recombinant Rat Liver Fatty Acid-Binding Protein to Small Anionic Phospholipid Vesicles Results in Ligand Release: A Model for Interfacial Binding and Fatty Acid Targeting, *Biochemistry 38*, 16932−16940.
27. Agasøster, A. V., Halskau, Ø., Fuglebakk, E., Frøystein, N., Muga, A., Holmsen, H., and Martínez, A. (2003) The interaction of peripheral proteins and membranes studied with α-lactalbumin and phospholipid bilayers of various compositions, *J. Biol. Chem. 278*, 21790−21797.
28. Sanghera, N., and Pinheiro, T. J. T. (2000) Unfolding and refolding of cytochrome c driven by the interaction with lipid micelles, *Protein Sci. 9*, 1194−1202.
29. Andrade, S. M., Carvalho, T. I., Viseu, M. I., and Costa, S. M. B. (2004) Conformational changes of β-lactoglobulin in sodium bis-(2-ethylhexyl) sulfosuccinate reverse micelles: A fluorescence and CD study, *Eur. J. Biochem. 271*, 734−744.
30. Banuelos, S., and Muga, A. (1995) Binding of molten globule-like conformations to lipid bilayers. Structure of native and partially folded α-lactalbumin bound to model membranes, *J. Biol. Chem. 270*, 29910−29915.
31. Banuelos, S., and Muga, A. (1996) Structural requirements for the association of native and partially folded conformations of α-lactalbumin with model membranes, *Biochemistry 35*, 3892−3898.
32. Brown, E. M., Carroll, R. J., Pfeffer, P. E., and Sampugna, J. (1983) Complex formation in sonicated mixtures of β-lactoglobulin and phosphatidylcholine, *Lipids 18*, 111−118.
33. Bos, M. A., and Nylander, T. (1996) Interaction between β-lactoglobulin and phospholipids at the air/water interface, *Langmuir 12*, 2791−2797.
34. Cornell, D. G., and Patterson, D. L. (1989) Interaction of phospholipids in monolayers with β-lactoglobulin adsorbed from solution, *J. Agric. Food Chem. 37*, 1455−1459.
35. Nolan, V., Perduca, M., Monaco, H. L., Maggio, B., and Montich, G. G. (2003) Interactions of chicken liver basic fatty acid-binding protein with lipid membranes, *Biochim. Biophys. Acta 1611*, 98−106.
36. Wootan, M. G., Bernlohr, D. A., and Storch, J. (1993) Mechanism of fluorescent fatty acid transfer from adipocyte fatty acid binding protein to membranes, *Biochemistry 32*, 8622−8627.
37. Kobayashi, T., Ikeguchi, M., and Sugai, S. (2000) Molten globule structure of equine β-lactoglobulin probed by hydrogen exchange, *J. Mol. Biol. 299*, 757−770.

BI602483P